

Article

Additive Manufacturing of Silicon Nitride Ceramic Floatation Spheres with Excellent Mechanical Properties

Hai Qi, Chenggui He, Peizhi Zhang *, Weiyue Han, Fangquan Guo, Fen Wu and Miaofeng Du

Shanghai Key Laboratory of Engineering Materials Application and Evaluation, Shanghai Research Institute of Materials, Shanghai 200437, China

* Correspondence: zhangpeizhi@srin.com.cn; Tel.: +86-021-6553-3030

Received: 2 August 2019; Accepted: 22 August 2019; Published: 24 August 2019



Abstract: Silicon nitride (Si_3N_4) ceramic materials are increasingly being used in deep-sea pressure-resistant applications because of their high compressive strength-to-weight ratio. In the present study, Si_3N_4 ceramic floatation spheres with an outer diameter of approximately 101 mm are successfully batch produced and evaluated. The implementation method was to prepare Si_3N_4 ceramic hemispherical housings and pair them together. In order to improve the safety of the joint, the hemispherical Si_3N_4 housings were gradually thickened from 1.80 to 2.50 mm at the equator near the joining surface, based on a 3D model with additive manufacturing technology. The weight-to-displacement ratio of the prepared floatation sphere is approximately 0.34 g/cm^3 . The flexural strength, compressive strength of the material and the collapse strength of a number of Si_3N_4 floatation spheres were tested to be 1150, 3847, and 205 MPa, respectively, to confirm the reliability of the process. Additional sustained and cyclic hydrostatic pressure tests simulating the full ocean depth working conditions are carried out on several Si_3N_4 floatation spheres, which perform very well and do not fail.

Keywords: silicon nitride; additive manufacturing; pressure housings; floatation spheres; full ocean depth; mechanical properties

1. Introduction

Buoyancy modules and housings utilized in underwater vehicles demand deep-sea pressure-resistant materials with high compressive strengths and low densities to meet the requirements of water pressure resistance and reduce equipment weight. Ceramic materials have a great advantage as deep-sea pressure-resistant materials because of their high compressive strength-to-weight ratio relative to high-strength steels and titanium alloys. Alumina (Al_2O_3) ceramics were first used to produce hollow spheres as buoyancy modules [1–3] and external pressure housings for deep-sea vehicles [4]. However, compared to silicon nitride (Si_3N_4) ceramics (see in Table 1), Al_2O_3 ceramics are not the best choice in terms of high compressive strength and low density. Si_3N_4 ceramics have a high compressive strength-to-weight ratio and are, therefore, favored by many researchers. Takagawa [5] compared several structural ceramics, confirmed Si_3N_4 ceramics as the best material for autonomous underwater vehicle (AUV) pressure-resistant housing, and prepared a scale model for a pressure test of 118 MPa. In some studies [6–8], Si_3N_4 ceramics were used as pressure housings for ocean bottom seismometers, and a series of pressure tests were conducted to confirm their reliability.

In the production of Al_2O_3 ceramic floatation spheres [1–3], seamless hollow spheres were prepared by rotation casting and pressureless sintering after drying. However, for Si_3N_4 ceramics, the seamless hollow sphere greenbody is not available. It would be damaged in the high-temperature and

high-pressure conditions during gas pressure sintering, which is necessary to apply to acquire high strength Si_3N_4 materials [9]. Consequently, fabricating two hemispherical housings and joining them together is the best way to prepare Si_3N_4 ceramic floatation spheres at present. However, the presence of joints causes the ceramic spheres to fail at a lower pressure than it would in the absence of joints [10]. As explored by Yano and Takagawa [11], a tiny deformation of the circular joining surface might seriously deteriorate the collapse strength because of the small overlapping area at the joining part. Due to the poor machinability of the ceramic materials, it is very difficult to precisely control the pairing of the two hemispherical Si_3N_4 housings through machining, which will result in extremely high costs, especially for batch production. Nevertheless, with the development of preparation processes for ceramics, a novel technology—additive manufacturing (AM, also known as 3D printing)—makes batch production of the Si_3N_4 floatation spheres feasible.

Table 1. Comparison of material properties between Si_3N_4 and Al_2O_3 (commercial reference values).

Properties	Si_3N_4 (Gas Pressure Sintered)	Al_2O_3 (High Purity, $\geq 99\%$)
Density (g/cm^3)	3.2	3.9
Flexural Strength (3 point, MPa)	900–1200	300–500
Compressive Strength (MPa)	3000–4000	2000–3500
Fracture Toughness ($\text{MPa}\cdot\text{m}^{1/2}$)	6.5	4.0
Young's Modulus (GPa)	300	380
Poisson's Ratio	0.27	0.23

The ISO/ASTM 52900:2015 standard of AM technologies introduces AM as the process of joining materials layer upon layer based on a 3D model. Theoretically, AM can build a part from any 3D model without following traditional manufacturing methods. It not only has the advantage of reducing manufacturing costs but also gives designers greater freedom. Breddermann et al. [12] investigated the possibility of building pressure housings in the AM process, and they demonstrated that the housings could be produced even though the reliability still needed to be confirmed.

The aim of this paper is to prepare Si_3N_4 ceramic floatation spheres with the aid of AM technology, therefore reducing cost and making batch production more feasible. As mentioned above, the implementation method is to prepare Si_3N_4 ceramic hemispherical housings first and then pair them together. In this study, the adopted process, which was explored by Deckers et al. [13], Liu et al. [14], and Liu et al. [15] with Al_2O_3 materials, is powder-based selective laser sintering (P-SLS, which belongs to indirect AM technologies as reviewed by Zocca et al. [16]) combined with cold isostatic pressing. The specific processing flow chart of preparing Si_3N_4 ceramic floatation spheres [17] is schematically shown in Figure 1. In addition, the flexural strength, compressive strength of the Si_3N_4 ceramic material, and collapse strength of a number of Si_3N_4 ceramic floatation spheres are tested to confirm the reliability of the process.

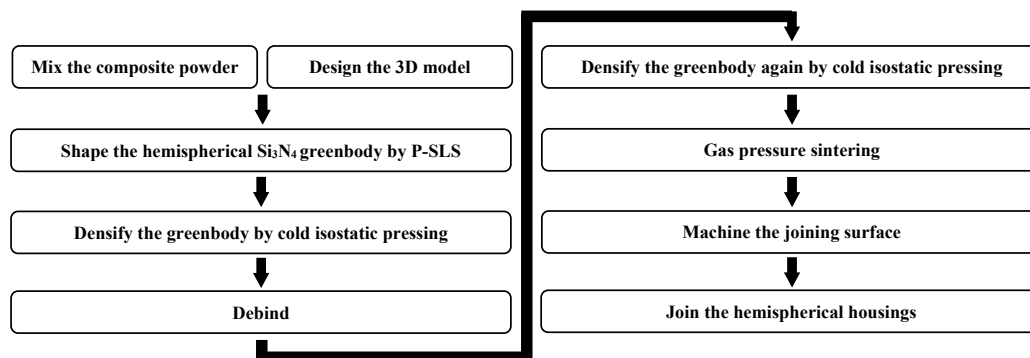


Figure 1. Preparation process of Si_3N_4 ceramic floatation spheres.

2. Materials and Methods

2.1. Composite Powder Preparation

The raw material was spray granulated [18] Si_3N_4 ceramic powder (provided by UBE Co., Tokyo, Japan, particle size: 50–100 μm) and was mechanically mixed with 20 wt% of epoxy resin powder (provided by Guangzhou Shinshi Metallurgy and Chemical Company LTD., Guangzhou, China, SH-E50) as a binder phase in a V-type mixer for printing.

2.2. Description of the 3D Model

The technical sketch of the 3D model is shown in Figure 2. After shrinking by cold isostatic pressing and sintering, the wall thickness of the hemispherical housing was expected to be 1.8 mm, and the region near the joining surface was expected to gradually thicken to 2.5 mm, which was determined by the maximum roundness error of the circular joining surface (about 0.7 mm). The purpose of thickening the hemispherical housing at the equator region was to reduce the impact of deformation of the circular joining surface and to improve the safety factor of the joint.

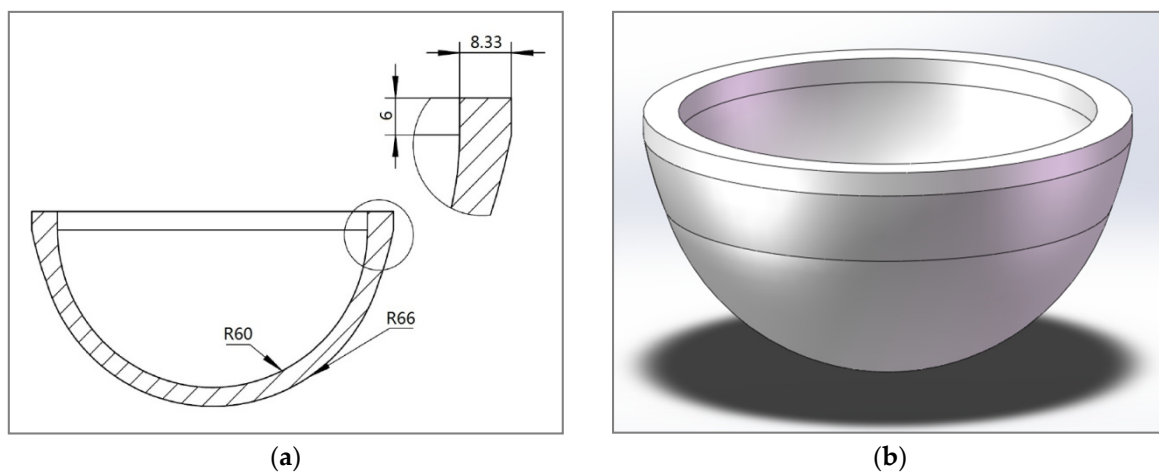


Figure 2. Technical sketch of the hemispherical greenbody. (a) CAD drawing; (b) 3D model.

2.3. Powder-Based Selective Laser Sintering

The hemispherical housing greenbodies were printed using a HRPS-IV SLS system (made by Huazhong University of Science and Technology, Wuhan, China) equipped with a 55 W CO_2 laser with a wavelength of 10.6 μm and a laser beam diameter of 200 μm . The laser power, scan speed, scan spacing, and layer thickness were 7.7 W, 2500 mm/s, 200 μm , and 100 μm , respectively.

2.4. Cold Isostatic Pressing and Debinding

The hemispherical housing greenbodies were cold isostatically pressed for 2 min at 260 MPa and then debinded for 2 h at 500 $^{\circ}\text{C}$. After debinding, cold isostatic pressing was conducted again on the greenbodies.

2.5. Sintering, Machining, and Joining

The debinded and cold isostatically pressed hemispherical housing greenbodies were sintered for 1 h at 1750 $^{\circ}\text{C}$ in 5 MPa of N_2 . Then, the joint surface of the sintered hemispherical housing was machined by grinding and polished with diamond paste of 0.5 μm . The joining of the hemispherical housings was carried out at a temperature of 1550 $^{\circ}\text{C}$ for 1 h in 0.1 MPa of N_2 .

2.6. Measurements and Test Procedure

The wall thickness of the hemispherical housings was measured by a micrometer (made by Shanghai Tool Works Co., LTD., Shanghai, China). The density of the resulting ceramic materials and the weight-to-displacement ratio of the floatation spheres were determined through the Archimedes method by an electronic balance (MP21001, made by Shanghai Sunny Hengping Scientific Instrument Co., LTD., Shanghai, China). The microstructure of the hemispherical housings in different processes was observed by scanning electron microscopy (SEM, VEGA 3 SBU, made by TESCAN, Brno, Czech). The joining status of the hollow spheres was observed by industrial computed tomography (CT, V|tome|x, made by GE, Boston, MA, USA).

The flexural strength (three-point) σ_F of the Si_3N_4 material was tested on sixteen $3 \times 4 \times 38 \text{ mm}^3$ samples (surface finished by grinding and polishing) at room temperature to evaluate the quality of the material. The calculation formula is

$$\sigma_F = \frac{3FL}{2bd^2} \quad (1)$$

where F is the fracture load, L is the fixture outer span (30 mm), b is the specimen width, and d is the specimen thickness. The Weibull modulus m was also calculated.

The compressive strength σ_C of the Si_3N_4 material was tested on ten $5 \times 5 \times 12.5 \text{ mm}^3$ samples (surface finished by grinding and polishing) at room temperature to provide data to predict the collapse strength of the floatation spheres. The calculation formula is

$$\sigma_C = \frac{P}{A} \quad (2)$$

where P is the compressive breaking load, and A is the specimen sectional area.

The collapse strength of the Si_3N_4 ceramic floatation spheres was tested in a 500 MPa rated pressure tank (LDJ180-250-500, made by MUCH Machinery Co., LTD., Foshan, China). The pressure was read with a type PTB702 pressure sensor (accuracy 1.2 MPa, made by Guangzhou Compass Sensor Instrument Co., LTD., Guangzhou, China). In addition, sustained and cyclic hydrostatic pressure tests were performed.

3. Results and Discussion

3.1. Preparation

Six hemispherical housings as a batch were printed by the SLS system based on the 3D model, as shown in Figure 3a. During printing, the epoxy resin powder was selectively melted by a laser light to bond the Si_3N_4 ceramic particles together to form parts. After removing the non-sintered composite powder, which could be reused, the greenbodies were taken out from the powder bed, as shown in Figure 3b.



Figure 3. (a) Printing the hemispherical greenbodies in the additive manufacturing (AM) equipment, and (b) the printed hemispherical greenbodies.

Figure 4a shows that the Si_3N_4 particles (spray granulated) adhered to each other with epoxy resin after printing. The loose structure of the printed greenbody was also observed. Since the density and uniformity of the greenbodies shaped by P-SLS were too low to obtain a high quality sintered body, cold isostatic pressing was applied to improve the strength and reliability of the material. Then, the greenbodies were debinded to remove the epoxy resin. Figure 4b shows the microstructure of the first cold isostatic pressed and debinded greenbody. Notably, lots of pores were generated in removing the high-content binder. In order to eliminate the pores, cold isostatic pressing was applied again to further improve the density and strength of the greenbodies. After the second cold isostatic pressing, the greenbody was firmer and much more uniform (see Figure 4c).

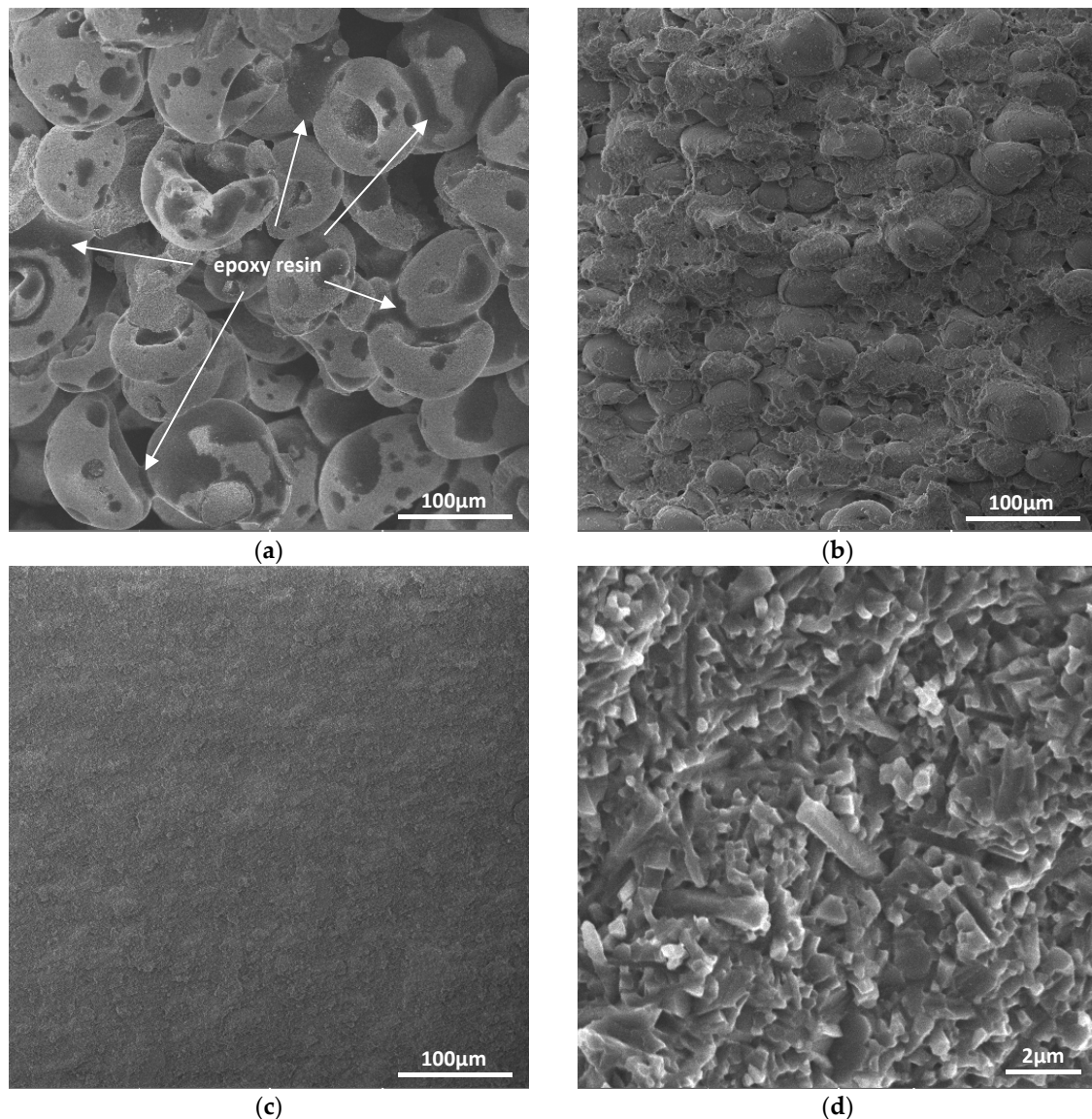


Figure 4. SEM micrographs of the hemispherical housings in different processes. (a) The printed greenbody before cold isostatic pressing CIP, (b) the first CIPed and debinded greenbody, (c) the second CIPed greenbody, and (d) the sintered Si_3N_4 body.

After cold isostatic pressing and debinding, the greenbodies were gas pressure sintered. Figure 4d shows the micrograph of the sintered Si_3N_4 body. The elongated rod-like grains provide toughening mechanisms that make Si_3N_4 materials have better mechanical properties than Al_2O_3 . The density of the sintered Si_3N_4 materials was measured to be 3.23 g/cm^3 , and the porosity was close to 0% according

to the theoretical density of the material, which means the ceramic materials had no pore defects. Next, the sintered hemispherical housings were machined and polished to prepare for joining together, as shown in Figure 5a. According to quite a few bonding phenomena, which were often observed between samples in contact with each other in some heat treatment experiments of Si_3N_4 ceramics, the hemispherical housings were joined at a high temperature (1550 °C) with a graphite fixture, as shown in Figure 5b. The advantage of heat joining is that it is much more durable than joining with organic adhesives. Heat treatment can also eliminate the stress concentration on the joining surface. In addition, in order to avoid water penetrating into the seam of the joined housings in deep-sea, high-pressure conditions, the seam was coated with carbon fiber material to seal and protect the interface, as shown in Figure 5c.

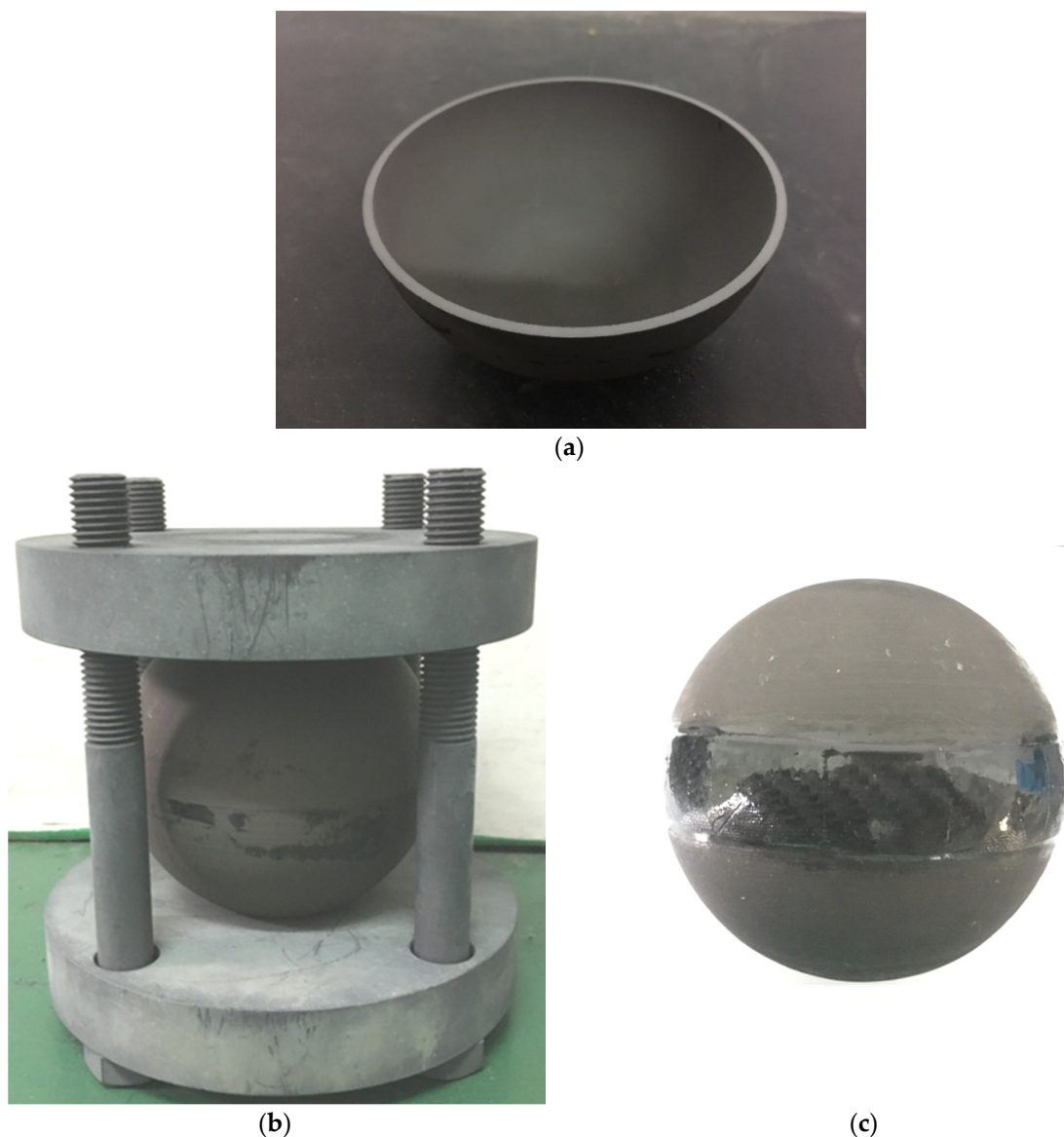


Figure 5. (a) A sintered and machined Si_3N_4 housing, (b) the graphite fixture for joining, and (c) a floatation sphere coated with the carbon fiber material.

This study prepared seventeen Si_3N_4 ceramic floatation spheres for pressure tests, sixteen samples for testing the flexural strength of the Si_3N_4 material, and ten samples for testing the compressive strength of the Si_3N_4 material.

3.2. Evaluation

The wall thickness distribution of the hemispherical housing after sintering and machining is shown in Figure 6. The wall thickness of the measured hemispherical housing ranged from 1.77 ± 0.02 mm to 2.50 ± 0.06 mm, and the thickened region ranged from 1.80 ± 0.02 mm to 2.50 ± 0.06 mm. Wall thickness measurements were basically consistent with the expected value, except for the pole location (2.06 mm), which might be attributed to the density inhomogeneity of the greenbody caused by the AM process. The diameter of the uncoated floatation spheres and the weight-to-displacement ratio of the coated floatation spheres were also measured, as shown in Tables 2 and 3.

A joined floatation sphere was scanned by industrial CT. No pores or other defects were observed in CT scanning (resolution 100 μ m). CT images show that the two hemispherical housings were joined well (Figure 7b), but slight misalignment between the two housings can be observed at the joint in Figure 7c, which should be the result of the roundness error of the circular joining surface.

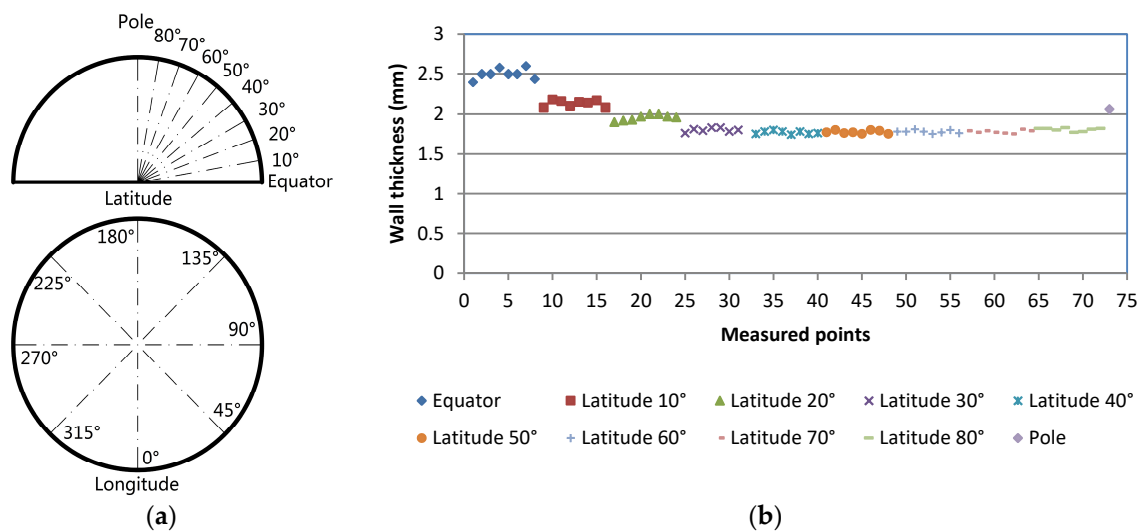


Figure 6. Wall thickness measurement results of a sintered and machined hemispherical housing. (a) Schematic diagram of wall thickness measured points of the hemispherical housing. (b) Measurement results.

Table 2. Diameter, weight-to-displacement ratio, and collapse strength of the Si₃N₄ floatation spheres.

Sample Number	Diameter (Uncoated, mm)	Weight-to-Displacement Ratio (Coated, g/cm ³)	Pressure (MPa)	Remarks
1	101.43	0.35	200	Collapsed
2	101.52	0.35	236	Collapsed
3	101.72	0.34	216	Collapsed
4	101.66	0.35	186	Collapsed
5	101.62	0.34	198	Collapsed
6	101.56	0.34	164	Collapsed
7	101.51	0.34	218	Collapsed
8	101.62	0.33	173	Collapsed
9	101.78	0.33	234	Collapsed
10	101.33	0.35	225	Collapsed
Average value	101.58	0.34	205	-

Table 3. Results of sustained and cyclic hydrostatic pressure tests.

Sample Number	Diameter (Uncoated, mm)	Weight-to-Displacement Ratio (Coated, g/cm ³)	Test Condition	Remarks
11	101.55	0.34	Sustained ¹	Not failed
12	101.31	0.35	Sustained	Not failed
13	101.79	0.33	Sustained	Not failed
14	101.83	0.33	Sustained	Not failed
15	101.42	0.35	Sustained	Not failed
16	101.63	0.33	Cyclic ²	Not failed
17	101.59	0.34	Cyclic	Not failed

¹ 145 MPa held for 10 h; ² 115 MPa held for 1 min and cycled 1000 times.

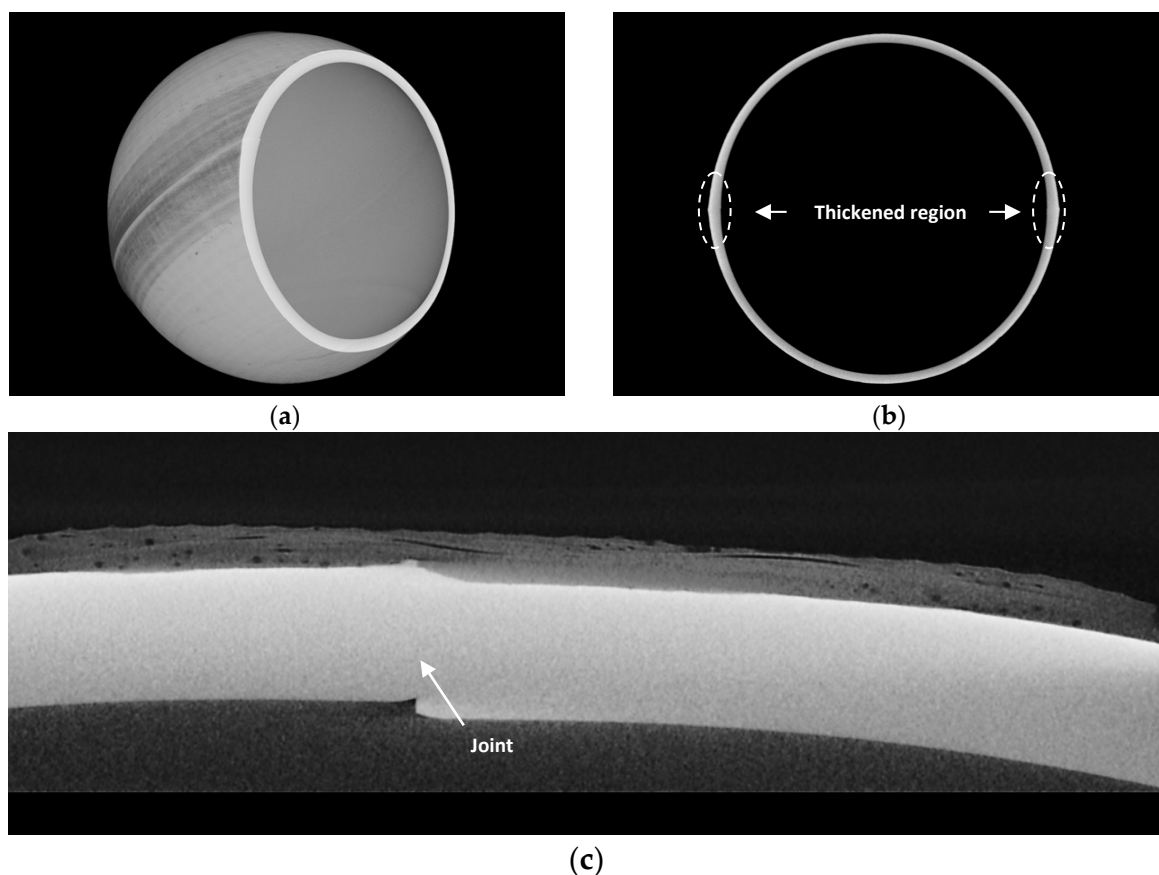


Figure 7. Industrial computed tomography (CT) images of a Si₃N₄ floatation sphere. (a,b) CT scanning. (c) Slight misalignment at the joint.

The flexural strength of the Si₃N₄ material was tested using sixteen samples ($3 \times 4 \times 38 \text{ mm}^3$, prepared with the same process as the hemispherical housings) at room temperature. The result is shown in Figure 8. The average value of the flexural strength was $1150 \pm 96 \text{ MPa}$, which means the Si₃N₄ material fabricated in this study achieved the same level as that of traditional processes (see in Table 1). The Weibull modulus m was calculated to be 11.8, which is close to the commercial material (Level I) in ASTM F2094. Therefore, the reliability of the material prepared by the process was confirmed.

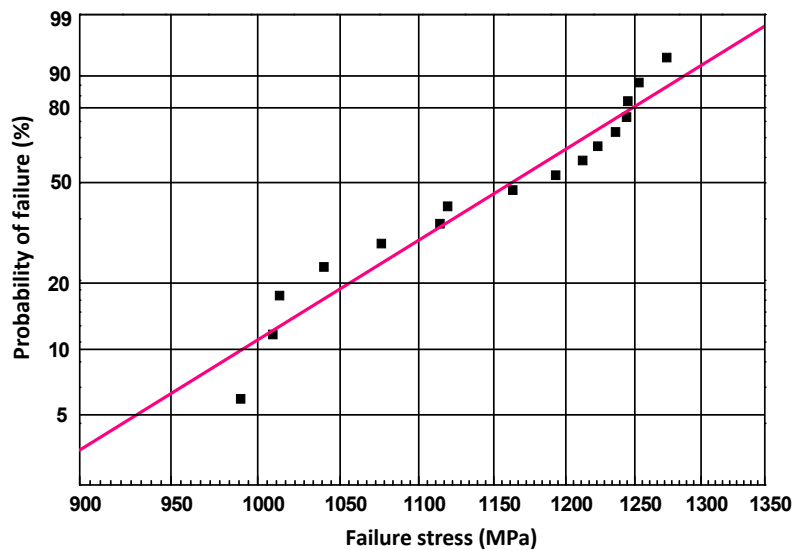


Figure 8. Weibull plot for flexural strength of the Si_3N_4 material fabricated based on powder-based selective laser sintering (P-SLS).

The compressive strength of the Si_3N_4 material was tested using ten samples ($5 \times 5 \times 12.5 \text{ mm}^3$, prepared with the same process as the hemispherical housings) at room temperature. The average value of the compressive strength was $3847 \pm 249 \text{ MPa}$ (ranged from 3467 MPa to 4239 MPa), which was also close to the Si_3N_4 material prepared by traditional processes (see in Table 1). As the compressive strength was tested, the collapse strength P_C of an ideal hollow sphere could be estimated by the formula [3,12]

$$P_C = \frac{2\sigma_C t}{r} \quad (3)$$

where σ_C is the compressive strength of the material, t is the wall thickness of the ceramic sphere, and r is the spherical radius. For the Si_3N_4 floatation spheres prepared in this study, t is 1.77 mm (the minimum value), r was 50.79 mm, and the calculated theoretical collapse strength of the floatation sphere was 268 MPa.

3.3. Pressure Tests

A total of seventeen Si_3N_4 floatation spheres prepared in this study were tested. Ten of them were tested to collapse, and the others were tested with sustained and cyclic hydrostatic pressure. The collapse strength ranged from 164 MPa to 236 MPa, and the average value was $205 \pm 24 \text{ MPa}$, as shown in Table 2. The results of the sustained and cyclic hydrostatic pressure tests are shown in Table 3. The test conditions were much closer to the actual working conditions, and all seven Si_3N_4 floatation spheres performed very well and did not fail.

The measured collapse strength was much lower than the theoretical value calculated above (268 MPa), which means there is still room to improve the shape's accuracy. For example, the sphericity of the hemispherical housings, which was not analyzed in detail in this study, has a large impact on collapse strength [19]. To improve the collapse strength and reduce data deviation, more details, such as sphericity, machining precision, and so on, in the process will be investigated and controlled in our future work.

For the Si_3N_4 floatation spheres prepared in this study, the safety factors of all the tested ten Si_3N_4 floatation spheres were high enough (from 1.5 to 2.2) for the full ocean depth conditions (maximum water pressure is 110 MPa). Therefore, we think this process of preparing Si_3N_4 floatation spheres was confirmed to be reliable for practical full ocean depth applications. Because of the high strength of the material, the performance of the Si_3N_4 floatation spheres was better than the seamless Al_2O_3 floatation spheres tested by Weston et al. [2]. Furthermore, based on the results in this study, it is clear that Si_3N_4

ceramic materials, with their high strength and low density, show great potential to serve in deep-sea pressure-resistant applications.

Since the reliability of the process adopted in this study was confirmed by testing the flexural strength, compressive strength of the material, and the collapse strength of the floatation spheres, it promises to develop the process in other deep-sea pressure-resistant applications and give ocean engineers greater freedom in designing pressure housings. It is worth noting that the process is not limited to Si_3N_4 ceramic materials. Other structural ceramic materials, such as Al_2O_3 , silicon carbide (SiC), zirconia (ZrO_2), zirconia toughened alumina (ZTA), and so on, are also available to prepare pressure housings for various requirements and working conditions.

4. Conclusions

This work demonstrates a new and feasible approach to realize batch production of deep-sea pressure-resistant floatation spheres with Si_3N_4 ceramic material. Based on AM technology, gradually thickened hemispherical Si_3N_4 housings (from 1.77 ± 0.02 mm to 2.50 ± 0.06 mm) were successfully prepared. After the joining surfaces were machined, the hemispherical housings were paired and joined to fabricate floatation spheres. In addition, the flexural strength (1150 ± 96 MPa) and the compressive strength (3847 ± 249 MPa) tested on samples prepared with the same process as the hemispherical housings confirmed the quality of the material. A series of pressure tests on a number of Si_3N_4 ceramic floatation spheres (the weight-to-displacement ratio was 0.34 ± 0.01 g/cm³) were conducted. Although the collapse strength (205 ± 24 MPa) of the floatation spheres was lower than the calculated theoretical value (268 MPa, according to the compressive strength of the material), it was high enough to meet the full ocean depth conditions. In the sustained and cyclic hydrostatic pressure tests, all tested floatation spheres performed well and did not fail.

Author Contributions: Conceptualization, P.Z.; methodology, P.Z. and H.Q.; validation, P.Z., H.Q., and C.H.; formal analysis, H.Q. and C.H.; investigation, H.Q., W.H., and F.W.; resources, F.G.; data curation, H.Q. and M.D.; writing—original draft preparation, H.Q.; writing—review and editing, P.Z. and C.H.; visualization, H.Q. and C.H.; supervision, P.Z.; project administration, F.G.; funding acquisition, P.Z.

Funding: This research was funded by the Scientific Research Program of Science and Technology Commission of Shanghai Municipality No. 14DZ1205900. The APC was funded by Shanghai Research Institute of Materials.

Conflicts of Interest: The authors declare no conflict of interest.

References

1. Stachiw, J.; Peters, D. Alumina Ceramic 10 in Flotation Spheres for Deep Submergence ROV/AUV Systems. In Proceedings of the OCEANS 2005 MTS/IEEE, Washington, DC, USA, 17–23 September 2005. [[CrossRef](#)]
2. Weston, S.; Stachiw, J.; Merewether, R.; Olsson, M.; Jemmott, G. Alumina ceramic 3.6 in flotation spheres for 11 km ROV/AUV systems. In Proceedings of the OCEANS 2005 MTS/IEEE, Washington, DC, USA, 17–23 September 2005. [[CrossRef](#)]
3. Jiang, B.; Blugan, G.; Sturzenegger, P.; Gonzenbach, U.; Mission, M.; Thornberry, J.; Stenerud, R.; Cartlidge, D.; Kuebler, J. Ceramic spheres—A novel solution to deep sea buoyancy modules. *Material* **2016**, *9*, 529. [[CrossRef](#)] [[PubMed](#)]
4. Stachiw, J.; Peters, D.; McDonald, G. Ceramic External Pressure Housings for Deep Sea Vehicles. In Proceedings of the OCEANS 2006, Boston, MA, USA, 18–21 September 2006. [[CrossRef](#)]
5. Takagawa, S. New ceramic pressure hull design for deep water applications. In Proceedings of the OCEANS'10 IEEE Sydney, Sydney, Australia, 24–27 May 2010. [[CrossRef](#)]
6. Askawa, K.; Ito, M.; Hyakudome, T. Evaluation of small models of ceramic housings for 11,000 m ocean bottom seismometers. In Proceedings of the OCEANS'10 IEEE SYDNEY, Sydney, Australia, 24–27 May 2010. [[CrossRef](#)]
7. Askawa, K.; Hyakudome, T.; Yoshida, M.; Okubo, N.; Ito, M.; Terada, I. Ceramic pressure-tight housings for ocean-bottom seismometers applicable to 11-km water depth. *IEEE J. Ocean. Eng.* **2012**, *37*, 756–763. [[CrossRef](#)]

8. Maeda, Y.; Askawa, K.; Obana, K.; Terada, I. Super-deep-sea ocean bottom seismometers using ceramic spheres. In Proceedings of the 2013 IEEE International Underwater Technology Symposium (UT), Tokyo, Japan, 5–8 March 2013. [[CrossRef](#)]
9. Biswas, S.K.; Riley, F.L. Gas pressure sintering of silicon nitride—Current status. *Mater. Chem. Phys.* **2001**, *67*, 175–179. [[CrossRef](#)]
10. Weston, S.; Olsson, M.; Merewether, R.; Sanderson, J. Flotation in ocean trenches using hollow ceramic spheres. *Mar. Technol. Soc. J.* **2009**, *43*, 110–114. [[CrossRef](#)]
11. Yano, Y.; Takagawa, S. Exploratory study on engineering ceramics pressure hulls for deep-sea submergence services. *Mar. Technol. Soc. J.* **2005**, *39*, 49–55. [[CrossRef](#)]
12. Breddermann, K.; Drescher, P.; Polzin, C.; Seitz, H.; Paschen, M. Printed pressure housings for underwater applications. *Ocean Eng.* **2016**, *113*, 57–63. [[CrossRef](#)]
13. Deckers, J.; Shahzad, K.; Vleugels, J.; Kruth, J.P. Isostatic pressing assisted indirect selective laser sintering of alumina components. *Rapid Prototyp. J.* **2012**, *18*, 409–419. [[CrossRef](#)]
14. Liu, K.; Shi, Y.; Li, C.; Hao, L.; Liu, J.; Wei, Q. Indirect selective laser sintering of epoxy resin—Al₂O₃ ceramic powders combined with cold isostatic pressing. *Ceram. Int.* **2014**, *40*, 7099–7106. [[CrossRef](#)]
15. Liu, K.; Sun, H.; Shi, Y.; Liu, J.; Zhang, S.; Huang, S.; Wang, M. Research on selective laser sintering of Kaolin—Epoxy resin ceramic powders combined with cold isostatic pressing and sintering. *Ceram. Int.* **2016**, *42*, 10711–10718. [[CrossRef](#)]
16. Zocca, A.; Colombo, P.; Gomes, C.; Gunster, J. Additive manufacturing of ceramics: Issues, potentialities and opportunities. *J. Am. Ceram. Soc.* **2015**, *98*, 1983–2001. [[CrossRef](#)]
17. Zhang, P.; He, C.; Wu, F.; Han, W.; Guo, F.; Qi, H. Ceramic Hollow Buoyancy Balls and Method of Manufacture. China Patent CN108975937-A, 31 May 2017.
18. Lukasiewicz, S.J. Spray-drying ceramic powders. *J. Am. Ceram. Soc.* **1989**, *72*, 617–624. [[CrossRef](#)]
19. Zhao, M.; Zhang, X.; Feng, M.; Zhang, P.; He, C.; Qi, H.; Han, W.; Guo, F. Underwater implosion of silicon nitride ceramic flotation spheres. *Mar. Struct.* under review.



© 2019 by the authors. Licensee MDPI, Basel, Switzerland. This article is an open access article distributed under the terms and conditions of the Creative Commons Attribution (CC BY) license (<http://creativecommons.org/licenses/by/4.0/>).